Computer Physics Communications 276 (2022) 108330

Contents lists available at ScienceDirect

Computer Physics Communications

www.elsevier.com/locate/cpc

carlomat_4.0, a new version of the general purpose Monte Carlo program ☆,☆☆

Karol Kołodziej

Institute of Physics, University of Silesia, ul. 75 Pułku Piechoty 1, PL-41500 Chorzów, Poland

ARTICLE INFO

Article history:
Received 8 April 2021
Received in revised form 8 December 2021
Accepted 25 February 2022
Available online 8 March 2022

Dataset link: 10.17632/9rx84cpvwc.1

Keywords:
General purpose program
Monte Carlo simulations
Automatic code generation
Electron-positron colliders
LHC

ABSTRACT

A new version of the general purpose Monte Carlo program carlomat is presented that substantially improves efficiency of the phase space integration by automatic inclusion of parameterizations which map away the t-channel poles and peaks due to soft and collinear photon or gluon emission. The quadruple precision versions of the routines for computation of the helicity amplitudes and phase-space parameterizations have been written and calls to them implemented in the code generation part of the program. This allows to better control numerical stability of the Monte Carlo programs generated, in particular for reactions with a virtual photon or gluon exchange in the t-channel. A new option of generating s-channel kinematics has been added which takes into account peaks due to Feynman propagators of intermediate bosons which decay into on shell final state particles, or of the top quark. It speeds up both the compilation and execution time of the Monte Carlo programs with respect to the kinematics based on topologies of the Feynman diagrams used in versions 2 and 3 of carlomat. To further speed up the execution time, the main routine of the Monte Carlo program has been supplemented with the Message Passing Interface which allows to run the program parallelly on several processors.

Program summary

Program Title: carlomat, version 4.0
CPC Library link to program files: https://doi.org/10.17632/9rx84cpvwc.1
Developer's repository link: https://www.kk.us.edu.pl/carlomat.html
Licensing provisions: GPLv3
Programming language: Fortran 90/95
Supplementary material: 'instructions.pdf'
Journal reference of previous version: Comput. Phys. Commun. 196 (2015) 563
Does the new version supersede the previous version?: Yes
Reasons for the new version: Efficient integration over a multi particle phase space can be a challenging task. Phase space parameterizations allowing to smoothen t-channel poles, or peaks due to soft and collinear photon or gluon emission, which were not taken into account in former versions of carlomat, are now included in the multichannel Monte Carlo integration routine automatically generated by the program. This allows to obtain more reliable predictions for quite a number of reactions that are of interest, either as signal or potential sources of background, both in high or low energy particle colliders.
Summary of revisions: Phase space integration routines, originally developed in Phys. Rev. D43 (1991) 3619 and Comput. Phys. Commun. 159 (2004) 106, have been brought to the form suitable for implementation in the general purpose Monte Carlo (MC) program. The code generation part of carlomat has been appropriately modified in order to include new phase space parameterizations in the automatically generated multichannel MC integration routine. Quadruple precision versions of the routines for computation of the helicity amplitudes and phase-space parameterizations have been written and calls to them implemented in the code generation part of carlomat. A number of new options have been introduced in the program which allow to control generation of the multichannel integration routine and the process of MC integration. Among them a new option of generating s-channel kinematics has been added which takes into account peaks due to Feynman propagators of intermediate bosons

☆ The review of this paper was arranged by Prof. Z. Was.
☆☆ This paper and its associated computer program are available via the Computer Physics Communications homepage on ScienceDirect (http://www.sciencedirect.com/science/journal/00104655).

E-mail address: karol.kolodziej@us.edu.pl.

https://doi.org/10.1016/j.cpc.2022.108330

which decay into on shell final state particles, or of the top quark. It speeds up both the compilation and execution time of the Monte Carlo programs with respect to the kinematics based on topologies of the Feynman diagrams used in versions 2 and 3 of the program. To further speed up the execution time, the main routine of the Monte Carlo program has been supplemented with the Message Passing Interface in order to allow for a parallel run of the program on several processors.

Nature of problem: Automatic generation of the MC codes for a wide class of reactions that can be measured in current and future accelerators.

Solution method: The `Fortran 90/95` MC programs are generated with a meta program that is also written in `Fortran 90/95`. All amenities of the former versions of `carlomat` are kept in the current version, too.

References

[1] K. Kołodziej, Comput. Phys. Commun. 196 (2015) 563.
[2] K. Kołodziej, M. Zrałek, Phys. Rev. D 43 (1991) 3619.
[3] K. Kołodziej, F. Jegerlehner, Comput. Phys. Commun. 159 (2004) 106.

1. Introduction

High energy particle colliders, a prominent example of which is the LHC, but also new colliders, whose projects have become more and more mature recently, as the electron–positron option of the Future Circular Collider (FCC–ee) [1] and Compact Linear Collider (CLIC) [2] at CERN, the International Linear Collider (ILC) [3] in Japan, or the Circular Electron–Positron Collider (CEPC) [4] in China, offer a unique possibility to test the nonabelian nature of gauge symmetry of the theory of fundamental interactions and mechanisms of the symmetry braking. These features of the theory can be directly tested in reactions in which a few heavy particles, as e.g. electroweak gauge bosons, heavy scalars or top quarks are produced at a time. The heavy particles are usually unstable and decay immediately leading to multi particle final states. The latter become also more and more relevant in the e^+e^- machines operating at low centre of mass energies. If one wants to determine hadronic contributions to vacuum polarization through dispersion relations from the energy dependence of the ratio of the cross section of $e^+e^- \to$ hadrons to the cross section of $e^+e^- \to \mu^+\mu^-$ with high precision then, in addition to the leading two pion production, the hadronic channels with several particles must be taken into account, too. Reliable theoretical predictions for aforementioned multi particle reactions can be obtained only within a fully automated approach, by using any of the following general purpose packages for Monte Carlo (MC) simulations: `MadGraph/MadEvent/HELAS` [5], `CompHEP/CalcHEP` [6], `ALPGEN` [7], `HELACPHEGAS` [8], `SHERPA/Comix` [9], `O'Mega/Whizard` [10], or `carlomat` [11], [12], [13]. Some packages, as `FeynArts/FormCalc` [14], `GRACE` [15], `MadGraph5_aMC@NLO` [16], `SHERPA 2.2` [17] and `HELAC-NLO` [18], offer a possibility of calculating NLO EW or QCD corrections.

`carlomat` [11] is a computer program written in Fortran 90/95 dedicated to automatic computation of the leading order (LO) cross sections of multiparticle reactions in the framework of the Standard Model and some effective models using diagrammatic approach. `carlomat_2.0` [12] has built-in interfaces to parton density functions. It generates a single phase space parameterization for the Feynman diagrams of the same topology, which substantially reduces size of the multi channel MC phase space integration routine with respect to the first version, where a different phase parameterization was generated for every Feynman diagram. It also includes the Cabibbo-Kobayashi-Maskawa mixing in the quark sector and some effective models such as scalar electrodynamics, the Wtb interaction with operators of dimension up to 5 and a general top–higgs coupling and some improvements concerning the colour matrix computation. `carlomat_3.0` [13] is dedicated to description of the processes of electron-positron annihilation to hadrons at low centre of mass energies. Version 3.1 offers a possibility of taking into account either the initial or final state radiation separately, or both at a time. It also allows to include the electromagnetic charged pion form factor for processes with charged pion pairs. All former versions of `carlomat`, as well as the current one, can be used as the MC generator of unweighted events.

Performing the phase space integration for such multiparticle reactions in an efficient way is a challenge indeed. In `carlomat` [11], this problem is tackled with the multichannel Monte Carlo (MC) integration routine generated automatically for a considered reaction. It combines phase space parameterizations corresponding to different topologies of the Feynman diagrams of the reaction, which take into account mappings of peaks related to the exchange of massless or massive unstable particles in the s-channel. However, parameterizations which map away the t-channel poles, or peaks due to soft and collinear photon or gluon emission, have not been included in the code generation routines of `carlomat` until now. As it will be clarified in the next section, in some phase space regions, the corresponding mappings require quadruple precision versions of routines for computation of the phase-space parameterizations and helicity amplitudes.

The paper is organized in the following way. In Section 2, the way in which the multichannel MC phase-space integration routine has been generated in former versions of `carlomat` is recalled. Newly implemented phase space parameterizations and related problems are discussed in Section 3, where also usage of the new program options is explained and sample results are presented. The summary and some remarks concerning the program distribution and preparation for running are given in Section 4.

2. Phase-space integration in `carlomat`

The phase-space integration element of reaction of the form

$$1 + 2 \to 3 + 4 + \ldots + n \tag{1}$$

is parameterized in the standard way

$$\mathrm{d}^{3n_\mathrm{f}-4}\mathrm{Lips} = (2\pi)^4\delta^{(4)}\Big(p_1+p_2-\sum_{i=3}^{n}p_i\Big)\prod_{i=3}^{n}\frac{\mathrm{d}^3p_i}{(2\pi)^3 2E_i}, \tag{2}$$

with $n_\mathrm{f}=n-2$ being the number of particles in the final state of (1). The basic idea behind the code generation for both the matrix element and phase space computation utilized in `carlomat` is to divide the final state particles $\{3,4,\ldots,n\}$ in two subsets, in accordance with a topology, or it would be better to say, shape of the Feynman diagram of the reaction. Let us denote the four momentum of the first subset by q_{i_1} and that of the second subset q_{i_2} and use consecutively the following identity

$$\int \mathrm{d}s_i \int \frac{\mathrm{d}^3q_i}{2E_i}\,\delta^{(4)}\left(q_i-q_{i_1}-q_{i_2}\right)=1, \qquad \text{where} \qquad E_i^2=s_i+\vec{q}_i^{\,2}, \tag{3}$$

until Eq. (2) is brought into the following form:

$$\mathrm{d}^{3n_\mathrm{f}-4}\mathrm{Lips} = (2\pi)^{4-3n_\mathrm{f}}\mathrm{d}^2l_0\mathrm{d}^2l_1\ldots\mathrm{d}^2l_{n-4}\mathrm{d}s_1\mathrm{d}s_2\ldots\mathrm{d}s_{n-4}. \tag{4}$$

In Eq. (4), $s_0=\left(q_{0_1}+q_{0_2}\right)^2=(p_1+p_2)^2=s$ and s_i, $i=1,\ldots,n-4$, are Lorentz invariants defined as $s_i=\left(q_{i_1}+q_{i_2}\right)^2$, and d^2l_i are 2-particle phase-space elements given by

$$\mathrm{d}^2l_i=\frac{|\vec{q}_{i_1}|}{4\sqrt{s_i}}\mathrm{d}\Omega_i, \qquad i=0,1,\ldots,n-4, \tag{5}$$

where $\mathrm{d}\Omega_i$ is the solid angle element of momentum $\vec{q}_{i_1}$ in the relative centre-of-mass system (c.m.s.), $\vec{q}_{i_1}+\vec{q}_{i_2}=\vec{0}$.

Invariants s_i of Eq. (4) are generated randomly, either according to the uniform distribution, or if necessary, mappings of the Breit-Wigner shape of the Feynman propagators of unstable particles and $\sim 1/s$ behaviour of the propagators of massless particles are performed. The physical limits of s_i's are automatically deduced from a topology of the Feynman diagram. An option is included in the program that allows to turn on the mapping if the particle decays into 2, 3, 4, ... on-shell particles. Different phase-space parameterizations obtained in this way can be used for testing purposes. It is obvious that only peaks related to the s-channel Feynman propagators can be mapped out in this way.

Denote a single phase-space parameterization generated according to Eq. (4) by $\mathrm{Lips}_a(x)$, where $x=(x_1,\ldots,x_{3n_\mathrm{f}-4})$, with x_i being random arguments, $x_i\in[0,1]$. The random numbers x are used to calculate the collection of the final state particle four momenta $\{p_3,\ldots p_n\}$. Therefore, parameterization $\mathrm{Lips}_a(x)$ will be referred to later on as the kinematic channel. Obviously, each phase space parameterization $\mathrm{Lips}_a(x)$ can be treated as a probability density function which satisfies the following normalization condition

$$\int_0^1 \mathrm{d}^{3n_\mathrm{f}-4}x\,\mathrm{Lips}_a(x)=\mathrm{vol}(\mathrm{Lips}). \tag{6}$$

All the parameterizations $\mathrm{Lips}_a(x)$, $a=1,\ldots,N$, generated by the program for a considered reaction are then automatically combined into a single multichannel probability density function

$$\mathrm{Lips}(x)=\sum_{a=1}^{N}w_a\mathrm{Lips}_a(x), \tag{7}$$

with non-negative weights w_a, $a=1,\ldots,N$, satisfying the condition

$$\sum_{a=1}^{N}w_a=1 \qquad \Leftrightarrow \qquad \int_0^1 \mathrm{d}^{3n_\mathrm{f}-4}x\,\mathrm{Lips}(x)=\mathrm{vol}(\mathrm{Lips}). \tag{8}$$

The actual MC integration is performed with the random numbers generated according to the probability density function $\mathrm{Lips}(x)$ of Eq. (7).

The MC integration in `carlomat` is performed iteratively. In the first step, the integral is scanned with a rather small number of random calls to the integrand, i.e. it is calculated N times, each time with a different phase-space parameterization $\mathrm{Lips}_a(x)$, resulting in the cross section $\sigma_a^{(0)}$. Weights $w_a^{(1)}$ of Eq. (7) for the first actual iteration are calculated according to the formula:

$$w_a^{(1)}=\frac{\sigma_a^{(0)}}{\frac{1}{N}\sum\limits_{b=1}^{N}\sigma_b^{(0)}}. \tag{9}$$

The weights $w_a^{(i+1)}$ for the $i+1$ iteration are then calculated according to the following formula:

$$w_a^{(i+1)}=\frac{\sigma_a^{(i)}}{\sum\limits_{b=1}^{N}w_b^{(i)}\sigma_b^{(i)}}. \tag{10}$$

This means that kinematic channels with small weights $w_a^{(i)}$ are chosen with low probability and will have small, or maybe even zero weights in all subsequent iterations. Weights $w_a^{(i)}$ are substituted to the multichannel probability density function (7) with which the

result of i-th iteration and the corresponding standard deviation are $\Delta\sigma^{(i)}$ are computed. The accumulated result for the cross section $\sigma_{\rm ac}$ and standard deviation $\Delta\sigma_{\rm ac}$ after $n_{\rm iter}$ iterations is calculated according to the following formula

$$\sigma_{\rm ac}=\frac{\sum\limits_{i=1}^{n_{\rm iter}}\sigma^{(i)}\left(\frac{\sigma^{(i)}}{\Delta\sigma^{(i)}}\right)^2}{\sum\limits_{i=1}^{n_{\rm iter}}\left(\frac{\sigma^{(i)}}{\Delta\sigma^{(i)}}\right)^2},\qquad \Delta\sigma_{\rm ac}=\frac{\sum\limits_{i=1}^{n_{\rm iter}}{\sigma^{(i)}}^2}{n_{\rm iter}\sum\limits_{i=1}^{n_{\rm iter}}\left(\frac{\sigma^{(i)}}{\Delta\sigma^{(i)}}\right)^2}, \tag{11}$$

which favours contributions from iterations with smaller variance. The accumulated result can be compared against the arithmetic mean value calculated as

$$\sigma_{\rm amv}=\frac{1}{n_{\rm iter}}\sum_{i=1}^{n_{\rm iter}}\sigma^{(i)},\qquad \Delta\sigma_{\rm amv}=\left[\frac{1}{n_{\rm iter}(n_{\rm iter}-1)}\sum_{i=1}^{n_{\rm iter}}(\Delta\sigma^{(i)})^2\right]^{\frac{1}{2}}. \tag{12}$$

If both results, $\sigma_{\rm ac}$ of (11) and $\sigma_{\rm amv}$ of (12), differ by less than one standard deviation, then the user can be satisfied with the result of integration. However, bigger discrepancies between the two results should be considered as a warning that something might be wrong with the integration procedure, in particular if one or a few results of individual iterations are much different from the average.

3. New developments in `carlomat`

As already mentioned in Section 2, the phase space parameterizations of Eq. (4), automatically generated and included in the multi-channel probability density function of Eq. (7) by all former versions of `carlomat`, are efficient in practice only for calculation of cross sections of reactions with s-channel peaks in their amplitudes. In this section, we describe parameterizations which map away peaks caused by the t-channel Feynman propagators, or soft and collinear photon/gluon emission from the initial- or final-state particles. They are also automatically included, together with the s-channel parameterizations, in the probability density function of Eq. (7), which should substantially facilitate the phase space integration for reactions involving such peaks. We also present a new way of generating kinematics responsible for mapping out the s-channel peaks which speeds up both the compilation and computation of the MC programs.

3.1. t-channel singularity

Reactions of the form:

$$e^+(p_1)+e^-(p_2)\to e^+(p_3)+e^-(p_4)+5+\ldots+n, \tag{13}$$

are typical in e^+e^- colliders. They receive contributions, among others, from the Feynman diagrams of the form depicted in Fig. 1, which possibly contain two t-channel peaks. In order to map out the singularity, the phase-space integration element of (13) is written in the following way:

$$\mathrm{d}^{3n_{\rm f}-4}{\rm Lips}=(2\pi)^{4-3n_{\rm f}}\mathrm{d}s'\mathrm{d}PS_3(s,m_3^2,m_4^2,s')\mathrm{d}PS_{n_{\rm f}-2}(s',m_5^2,\ldots,m_n^2), \tag{14}$$

where identity (3) has been used and

$$\mathrm{d}PS_3(s,m_3^2,m_4^2,s')=\delta^{(4)}\Big(p_1+p_2-p_3-p_4-p'\Big)\frac{\mathrm{d}p_3^3}{2E_3}\frac{\mathrm{d}p_4^3}{2E_4}\frac{\mathrm{d}p'^3}{2E'}, \tag{15}$$

$$\mathrm{d}PS_{n_{\rm f}-2}(s',m_5^2,\ldots,m_n^2)=\delta^{(4)}\Big(p'-\sum_{i=5}^{n}p_i\Big)\prod_{i=5}^{n}\frac{\mathrm{d}p_i^3}{2E_i}, \tag{16}$$

are 3- and $(n_{\rm f}-2)$-particle phase-space elements, respectively, as defined by Eq. (2), with the corresponding powers of (2π) in Eqs. (15) and (16) included in the common factor on the right hand side of Eq. (14) and in Eq. (15), $E'=\sqrt{s'+\vec{p}\,'^2}$.

The t-channel singularity can be mapped out by writing the 3-particle phase-space element of Eq. (15) in the following form

$$\mathrm{d}PS_3(s,m_3^2,m_4^2,s')=\frac{1}{8}\delta(\sqrt{s}-E_3-E_4-E')\frac{|\vec{p}_3||\vec{p}_4|}{E'}\mathrm{d}E_3\mathrm{d}E_4\mathrm{d}\Omega_3\mathrm{d}\Omega_4, \tag{17}$$

where $E'=\sqrt{s'+(\vec{p}_3+\vec{p}_4)^2}$ and all kinematic variables on the r.h.s. are define in c.m.s. Introducing dimensionless variables $x=2E_3/\sqrt{s}$ and $y=2E_4/\sqrt{s}$, Eq. (17) can be written in the following way [19]:

$$\mathrm{d}PS_3(s,m_3^2,m_4^2,s')=\frac{1}{8}\frac{|\vec{p}_3||\vec{p}_4|}{2-x+y\frac{|\vec{p}_3|}{|\vec{p}_4|}\cos\theta_{34}}\mathrm{d}x[\delta(y-y_+)+\delta(y-y_-)]\mathrm{d}y\mathrm{d}\Omega_3\mathrm{d}\Omega_4, \tag{18}$$

where $\mathrm{d}\Omega_i=\mathrm{d}\cos\theta_i\mathrm{d}\varphi_i$, $i=3,4$, are the solid angle elements of momenta $\vec{p}_3$ and $\vec{p}_4$ of particles 3 and 4 and

$$\cos\theta_{34}=\cos\theta_3\cos\theta_4+\sin\theta_3\sin\theta_4\cos(\varphi_3-\varphi_4). \tag{19}$$

In Eq. (18), $y_\pm$ are the solutions, possibly 2, of the energy conservation equation, as defined by zero of the Dirac delta of Eq. (17)

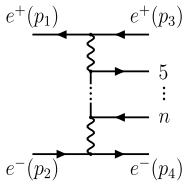

Fig. 1. Feynman diagram of reaction (13) containing double t-channel singularity.

$$\sqrt{s}-E_3-E_4-E'=\sqrt{s}-\frac{\sqrt{s}}{2}x-\frac{\sqrt{s}}{2}y - \left[s'+\frac{s}{4}x^2-m_3^2+\frac{s}{4}y^2-m_4^2+2\sqrt{\frac{s}{4}x^2-m_3^2}\sqrt{\frac{s}{4}y^2-m_4^2}\cos\theta_{34}\right]^{1/2}=0. \tag{20}$$

The random variables of Eqs. (14) and (18) are generated in a similar way as in [20], with some minor modifications, i.e.

- s' is generated according to $\sim 1/s'$ distribution.
- x is generated according to $\sim 1/(1-x)$ distribution.
- Azimuthal angles φ_3 and φ_4 are generated according to the uniform distribution.
- $\cos\theta_3 \in [-\cos\theta_{\rm cut}, \cos\theta_{\rm cut}]$ is generated according to

$$\sim \frac{1}{1-\beta_3\cos\theta_3}, \qquad \text{with} \qquad \beta_3=\frac{2|\vec{p}_1||\vec{p}_3|}{2E_1E_3-m_3^2}. \tag{21}$$

- $\cos\theta_4 \in [-\cos\theta_{\rm cut}, \cos\theta_{\rm cut}]$ is generated according to

$$\sim \frac{1}{a_4+\cos\theta_4}, \qquad \text{where} \qquad a_4=\frac{2E_2\tilde{E}_4-m_4^2}{2|\vec{p}_2|\sqrt{\tilde{E}_4^2-m_4^2}} \tag{22}$$

  and $\tilde{E}_4$, its choice being explained below, is used in a_4 instead of energy E_4 of particle 4.
- The $(n_{\rm f}-2)$-particle phase-space element of Eq. (16) is generated in a way similar to the s-channel phase-space generation of `carlomat`.

The energy E_4 of particle 4 is not known until $\cos\theta_4$ has been generated and $\cos\theta_{34}$, which is needed in Eq. (20), calculated according to Eq. (19). Therefore, in Eq. (22), $\tilde{E}_4$ is used instead of E_4. It is chosen as the solution of Eq. (20) for $\cos\theta_{34}=-1$, which corresponds to the collinear singularity being most pronounced. Then $\cos\theta_{34}$ is calculated according to Eq. (19) and substituted to Eq. (20). If there is no solution for y, then $\mathrm{d}^{3n_{\rm f}-4}$Lips of Eq. (14) is set to 0. If two solutions $y_\pm$ exist, then one of them is chosen randomly and the phase-space $\mathrm{d}^{3n_{\rm f}-4}$Lips is multiplied by a factor 2.

3.2. Photon or gluon emission

Consider the reaction of the photon or gluon radiation of the following form:

$$1+2\to 3+4+\ldots+n+\gamma, \tag{23}$$

with the number of final state particles $n_{\rm f}$ given by $n_{\rm f}=n+1-2=n-1$. In order to map out soft and collinear singularities of the initial state radiation amplitudes, we parameterize the phase-space element of (23) in the following way

$$\mathrm{d}^{3n_{\rm f}-4}\mathrm{Lips}=\frac{1}{2}(2\pi)^{4-3n_{\rm f}}E_\gamma\mathrm{d}E_\gamma\mathrm{d}\Omega_\gamma\mathrm{d}PS_{n_{\rm f}-1}(s',m_3^2,\ldots,m_n^2), \tag{24}$$

where E_γ and $\mathrm{d}\Omega_\gamma=\mathrm{d}\cos\theta_\gamma\mathrm{d}\varphi_\gamma$ are the energy and solid angle element of the photon in the c.m.s., respectively, $\mathrm{d}PS_{n_{\rm f}-1}(s',m_3^2,\ldots,m_n^2)$ is defined according to Eq. (16), with an obvious change of notation, and after emission of the photon of four momentum p_γ from the initial state particle, the reduced c.m.s. energy squared is given by $s'=(p_1+p_2-p_\gamma)^2=s-2\sqrt{s}E_\gamma$.

The random variables of Eq. (24) are generated in the following way:

- E_γ is generated according to $\sim 1/E_\gamma$ distribution with the minimum photon energy $E_\gamma^{\rm cut}$.
- $\cos\theta_\gamma \in [-\cos\theta_\gamma^{\rm cut}, \cos\theta_\gamma^{\rm cut}]$ is generated according to

$$\sim \frac{1}{1-\beta^2\cos^2\theta_\gamma}, \qquad \text{with} \qquad \beta=\sqrt{1-\frac{4m^2}{s}},$$

  where equal masses of the initial state particles, $m_1=m_2=m$, have been assumed for the sake of simplicity.
- φ_γ is generated according to a uniform distribution.
- $\mathrm{d}PS_{n_{\rm f}-1}(s',m_3^2,\ldots,m_n^2)$ is generated in a way that takes into account peaks due to the s-channel Feynman propagators, as described by Eq. (4) and in a paragraph just below it.

Soft and collinear singularities of amplitudes of the final state radiation from either particle 3 or 4 of reaction (23) are treated with the following phase-space element parameterization

$$\begin{aligned} \mathrm{d}^{3n_\mathrm{f}-4}\mathrm{Lips} = (2\pi)^{4-3n_\mathrm{f}}\mathrm{d}s'\mathrm{d}s''\mathrm{d}PS_2(s,s',s'') \\ \times \mathrm{d}PS_3(s',m_3^2,m_4^2,0)\,\mathrm{d}PS_{n_\mathrm{f}-3}(s'',m_5^2,...,m_n^2), \end{aligned} \tag{25}$$

where $s' = (p_3+p_4+p_\gamma)^2$, $s'' = (p_5+...+p_n)^2$ and the 2-, 3- and $(n_\mathrm{f}-3)$-particle phase-space elements are defined appropriately according to Eq. (16). The 3-particle phase-space element on the r.h.s. of Eq. (25), corresponding to the photon radiation off particle 4, is parameterized by

$$\mathrm{d}PS_3(s',m_3^2,m_4^2,0) = \frac{1}{8}\mathrm{d}E_\gamma\,\mathrm{d}E_3\mathrm{d}\cos\theta_3\mathrm{d}\varphi_3\mathrm{d}\varphi_{37}, \tag{26}$$

where the random variables are generated in the same way as in a program `ee4f`γ [21], i.e.

- E_γ is generated according to $\sim 1/E_\gamma$, with the minimum photon energy E_γ^{cut} boosted to the c.m.s. of particles 3, 4 and γ.
- E_3 is generated according to

$$\sim \frac{1}{c_3 - E_3} \sim \frac{1}{p_4\cdot p_\gamma}.$$

- $\cos\theta_3$, φ_3 and φ_{37} are generated according to the uniform distribution.

3.3. Quadruple precision

Parameterizations (14), (24) and (25), which map away peaks due to the t-channel Feynman propagators, or soft and collinear photon or gluon emission from the initial- or final-state particles, may lead to numerical instabilities. The latter may occur in particular at high energies and small angles and their potential sources are the following. The final-state four momenta $p_1,...,p_\mathrm{f}$ of reactions (1), (13) or (23), generated randomly according to the probability density function $\mathrm{Lips}_b(x)$, must be used to calculate the normalization factors of all other densities $\mathrm{Lips}_a(x)$, $a=1,...,N$, of Eq. (7) in order to obtain proper phase-space normalization. To do so for any $a\neq b$, the necessary random variables $x=(x_1,...,x_{3n_\mathrm{f}-4})$ must be recalculated from the already generated four momenta $p_1,...,p_\mathrm{f}$. Obviously, this can also be done for $a=b$ and the value of $\mathrm{Lips}_b(x)$ obtained by this inversion can be compared to the original one with which the four momenta have been generated. Eventual discrepancies are recorded in the program output. Generation of $\cos\theta_3$ and $\cos\theta_4$ according to distributions (21) and (22), respectively, for reactions involving the t-channel poles may also become numerically unstable.

These problems can be circumvented either by expanding the appropriate formulae in relevant phase space regions into the Taylor series, cancelling leading terms analytically and performing computation with the double precision (DP) arithmetics, or by the use of quadruple precision (QP) arithmetics. In the new version of `carlomat`, both approaches are used, which gives a possibility of comparing the corresponding cross sections computed with the DP and QP precision arithmetics. The use of QP requires new versions of all routines for calculating both kinematics and the helicity amplitudes, which have been written and tested. However, it should be noted at this point that the corresponding MC programs in QP are much slower, typically by more than a factor 50, than those in the DP. Therefore, the QP arithmetics should be used rather to test if the corresponding DP code is good enough and not as an actual tool for the MC simulations. If a variable is close to a verge of it physical range then limited precision of the DP arithmetics may drive it out of the range and thus give a wrong result either for the phase space normalization or the matrix element. A number of criteria have been implemented in the program which set the phase normalization to zero in such cases. This means that such events do not terminate the program, but just do not contribute to the result. Whenever a random event is rejected a record of it is kept in the program output.

3.4. New s-channel integration routine

The multi channel MC integration routine automatically generated by versions 2 and 3 of `carlomat` combined the phase space parameterizations corresponding to different topologies and propagators of the Feynman diagrams. The number of such parameterizations may be very large for multiparicle reactions. Quite some care has been taken to combine those parameterizations in the integration routine in a way that makes its compilation at all possible. However, the corresponding compilation and execution time may become quite long.

The current version of the program offers a possibility of generating s-channel kinematics by taking into account peaks due to Feynman propagators of intermediate bosons which decay into on shell final state particles, or of the top quark. The corresponding kinematical routine is much shorter which speeds up both the compilation and execution time of the MC programs generated by `carlomat`. To this end a number of new subroutines have been written to compute the phase space normalization and generate the final state particle four momenta for reactions with 4, 5,..., 9 particles in the final state and calls to them have been generated in the code generation part of the program.

3.5. Parallelization of the MC program computation

To further speed up the execution time of the MC programs automatically generated by `carlomat`, the main routine of the MC computation part of the program `carlocom.f` has been supplemented with the Message Passing Interface (MPI) in order to allow for a parallel run of the program on several processors at a time. The corresponding new routine is named `carlocom_mpi.f`. With the use of MPI, the elapsed time of the MC program execution can be substantially shortened, i.e. in practice divided by the number of processor cores used. This scaling, however, is not ideal. How it actually works will be addressed in more detail in Section 3.7.

Table 1
LO cross sections of reaction (27) at $\sqrt{s} = 200$ GeV and $\sqrt{s} = 500$ GeV for 3 different ranges of the lepton–beam angle, computed with double and quadruple precision arithmetics. Uncertainties of the last digits are given in parentheses.

σ(200 GeV)	σ_{QP}(200 GeV)	σ(500 GeV)	σ_{QP}(500 GeV)
	$1^\circ < \theta(l, \text{beam}) < 179^\circ$		
14.48(6) pb	14.48(6) pb	3.048(29) pb	3.034(28) pb
	$0.001^\circ < \theta(l, \text{beam}) < 179.999^\circ$		
60.16(12) nb	60.17(12) nb	47.42(12) nb	47.39(12) nb
	$0.000001^\circ < \theta(l, \text{beam}) < 179.999999^\circ$		
252.2(4) nb	252.1(4) nb	282.4(5) nb	284.1(5) nb
	$0^\circ < \theta(l, \text{beam}) < 180^\circ$		
–	302.3(5) nb	–	404.5(7) nb

3.6. Use of new program options

All modifications described in this section can be easily controlled by a few new options which have been introduced in `carlomat.f`, the main routine of the code generation part of the program. Below we explain how they can be used and illustrate their effects with sample results in Section 3.5.

The use of the QP arithmetics is controlled with an option

```
iqprec=1 (yes)/else (no).
```

Compilation and computation of the generated MC kinematic routines might be very time consuming, therefore an option

`ischnl=1 (yes, generate kinematics based on topologies of the Feynman diagrams)/2 (yes, generate kinematics taking into account poles due to Feynman propagators of intermediate bosons which decay into on shell final state particles, or of the top quark)/else (no)?`

has been introduced which allows to change or discard generation of kinematic routines dedicated to integration of the s-channel peaks. Routines corresponding to `ischnl=1` have been automatically generated for any user selected reaction in all former versions of the program. Note, however, that if `ischnl=0` is chosen, then either of the two options `igchnl`, or `itchnl`, described below, must be set to a nonzero value, otherwise no kinematic routine will be generated and the program will be stopped.

Generation of kinematic routines dedicated to reactions with the t-channel photon or gluon exchange in reactions with two identical fermion-antifermion pairs, one in the initial state and the other in the final state, is controlled with an option

```
itchnl=1 (yes)/else (no).
```

Whether or not kinematics dedicated to a reaction of single photon or gluon radiation should be generated is controlled with an option

```
igchnl=1 (yes)/else (no).
```

It happens that the standard deviation of the MC integration becomes unexpectedly large just because the result of one particular iteration of Eqs. (11) substantially deviates from the results of all other iterations. Sometime the deviation is caused by just one or a few random events which due to numerical cancellations give unexpectedly large contribution to the integral. Therefore, an option has been introduced which allows to eliminate events whose contribution exceeds by more than a factor `mxfctr` the maximum of the cross section determined for all prior calls to the integrand in a given kinematic channel. It is specified with the assignment

```
mxfctr=1.d3
```

in `carlocom.f` of `mc_computation`. The actual value of `mxfctr` should be chosen *empirically*, such that the culprit-iteration is brought to the value not much different from other iterations. However, it is recommended to check by a comparison with the QP version of the program, if the rejected events do not influence much the result of the computation, say by more than one standard deviation of the MC integration.

To better control the MC integration process, a new option `irand` has been introduced both in `carlocom.f` and `carlocom_mpi.f` of `mc_computation` that allows to choose between the intrinsic random number generator of the Fortran compiler and `ranlux` [22]. Another new option, `iprind`, allows to print results computed by individual processes which are run in the parallel version of the MC program.

3.7. Sample results

For the sake of illustration, we show below a sample of results obtained with the use of current version of `carlomat` and new options described in Section 3.4. The physical input parameters used in the computation are defined in module `inprms` in directory `mc_computation`.

To demonstrate the use of the t-channel kinematics and potential necessity of the QP arithmetics we show in Table 1 the leading order (LO) cross sections of the reaction

$$e^+e^- \to e^+e^-\mu^+\mu^- \tag{27}$$

Table 2
LO cross sections of reaction (30) at $\sqrt{s} = 200$ GeV and $\sqrt{s} = 500$ GeV for $E_\gamma > 1$ GeV and different angular cuts. Uncertainties of the last digits are given in parentheses.

Angular cuts		σ(200 GeV)	σ(500 GeV)
$1^\circ < \theta(\gamma, \text{beam}) < 179^\circ$,	$\theta(\gamma, l) > 1^\circ$	7.42(2) fb	2.30(1) fb
$1^\circ < \theta(\gamma, \text{beam}) < 179^\circ$,	$\theta(\gamma, l) > 0^\circ$	8.10(2) fb	2.66(1) fb
$0^\circ < \theta(\gamma, \text{beam}) < 180^\circ$,	$\theta(\gamma, l) > 1^\circ$	14.95(4) fb	4.87(3) fb
$0^\circ < \theta(\gamma, \text{beam}) < 180^\circ$,	$\theta(\gamma, l) > 0^\circ$	15.84(4) fb	5.34(3) fb

Table 3
LO cross sections (in fb) of reaction (30) at $\sqrt{s} = 200$ GeV and $\sqrt{s} = 500$ GeV for $1^\circ < \theta(\gamma, \text{beam}) < 179^\circ$, $\theta(\gamma, l) > 1^\circ$ and $E_\gamma > 1$ GeV and corresponding numbers of calls to the integrand. Δt_1 (Δt_4) is the elapsed time of calculation of both σ(200 GeV) and σ(500 GeV) in a single core (4-cores) mode. Uncertainties of the last digits are given in parentheses.

	$n_{\text{cores}} = 1$			$n_{\text{cores}} = 4$		
	Δt_1	σ(200 GeV)/N	σ(500 GeV)/N	Δt_4	σ(200 GeV)/N	σ(500 GeV)/N
IFRNG	24′42″	7.467(35)/17.7M	2.282(20)/17.2M	6′19″	7.412(37)/17.9M	2.283(20)/17.1M
`ranlux`	25′18″	7.478(43)/17.8M	2.275(15)/17.4M	6′32″	7.447(44)/17.9M	2.295(22)/17.1M
IFRNG	241′26″	7.509(16)/178M	2.318(7)/172M	64′52′	7.517(18)/178M	2.324(10)/173M
`ranlux`	246′34″	7.531(17)/177M	2.311(9)/172M	65′42″	7.497(19)/177M	2.305(8)/172M

at $\sqrt{s} = 200$ GeV and $\sqrt{s} = 500$ GeV for 4 different ranges of the lepton–beam angle $\theta(l, \text{beam})$. We see that the cross sections σ and σ_{QP} calculated with the DP (`iqprec=0`) and QP (`iqprec=1`) arithmetics, respectively, agree well, i.e., within one standard deviation shown in parentheses as uncertainty of the last decimals, for $1^\circ < \theta(l, \text{beam}) < 179^\circ$ and $0.001^\circ < \theta(l, \text{beam}) < 179.999^\circ$. The agreement is still satisfactory in the range $0.000001^\circ < \theta(l, \text{beam}) < 179.999999^\circ$ at $\sqrt{s} = 200$ GeV, but at $\sqrt{s} = 500$ GeV, there is already quite some discrepancy between σ and σ_{QP}. This is due to a certain number of random events rejected in the computation of the DP cross section, as discussed in Section 3.3. Among other criteria introduced to eliminate events for which some kinematic variables because of numerical cancellations are driven out of their physical limits, the following conditions in the kinematic routine that maps away the t-channel poles of reaction (27) are imposed

$$t_1 = (p_1 - p_3)^2 > t_1^{\max} = -m_1^2 \left[2 - \left(\frac{E_3}{E_1} + \frac{E_1}{E_3}\right)\right] \quad \Rightarrow \quad \mathrm{d}^{3n_{\mathrm{f}}-4}\mathrm{Lips} = 0, \tag{28}$$

$$t_2 = (p_2 - p_4)^2 > t_2^{\max} = -m_2^2 \left[2 - \left(\frac{E_4}{E_2} + \frac{E_2}{E_4}\right)\right] \quad \Rightarrow \quad \mathrm{d}^{3n_{\mathrm{f}}-4}\mathrm{Lips} = 0, \tag{29}$$

where p_1 (p_3) is the four momentum of the initial (final) state positron and p_2 (p_4) is the four momentum of the initial (final) state electron. However, if there is no cut on $\theta(l, \text{beam})$, conditions (28) and (29) are not enough any more and the DP precision cross sections σ become completely unreliable. Therefore they are not shown in Table 1.

Efficacy of kinematic routines dedicated to reactions of single photon radiation is illustrated in Table 2, where the cross sections of the reaction

$$e^+e^- \to \mu^+\mu^-\tau^+\tau^-\gamma \tag{30}$$

at $\sqrt{s} = 200$ GeV and $\sqrt{s} = 500$ GeV for $E_\gamma > 1$ GeV and with different cuts on the photon–beam and photon–lepton angles, $\theta(\gamma, \text{beam})$ and $\theta(\gamma, l)$ respectively, are shown. The QP results are not shown this time, as they are identical to those of the computation with DP arithmetics. The cross sections of reactions (27) and (30) agree well with those of `ee4f`γ [21], which in turn were thoroughly tested against results of programs by other authors, `EXCALIBUR` [23] and `RacoonWW` [24].

At this point, we would like to address the issue of computing time gain due to parallelization of the MC program. To this end the cross sections of the first row of Table 2 are recalculated with the MPI, once using 4 cores and the other time a single core only of a 4-core Intel i5-3470 3.2 GHz processor, which corresponds to setting `n_cores:=4` and `n_cores:=1`, respectively, in a makefile `mpi`. The MC integration is performed in 10 iterations with nominally 2×10^6 or 2×10^7 calls to the integrand and it is repeated with two different random number generators: the intrinsic Fortran random number generator (IFRNG) and `ranlux` [22], corresponding to `irand=1` and `irand=2` in `carlocom_mpi.f`. The cross sections are shown in Table 3 together with the actual number of calls to the integrand, i.e. after applying cuts and rejecting events being out of their allowed kinematical ranges. Also shown is the elapsed time Δt_1 (Δt_4) of calculation of both σ(200 GeV) and σ(500 GeV) in a single core (4-cores) mode. Note that Δt_1 is somewhat smaller than $4 \times \Delta t_4$, and the difference $4 \times \Delta t_4 - \Delta t_1$ is in a sense a measure of the non-parallelizable remnant of the program. The computing time can be further shortened if the s-channel kinematics is generated with an option `ischnl=2` instead of `ischnl=1` in `carlomat.f`. However, this particular option still needs more work before it becomes fully functional.

To further illustrate potential applications of the current version of `carlomat`, the LO cross sections of the following reactions

$$e^+e^- \to e^+e^-\pi^+\pi^-, \tag{31}$$

$$e^+e^- \to e^+e^-\pi^+\pi^-\gamma, \tag{32}$$

$$e^+e^- \to e^+e^-\mu^+\mu^-\pi^+\pi^-, \tag{33}$$

$$e^+e^- \to e^+e^-\mu^+\mu^-\pi^+\pi^-\gamma \tag{34}$$

$$e^+e^- \to be^+\nu_e\bar{b}e^-\bar{\nu}_e, \tag{35}$$

Table 4
LO cross sections of reactions (31)–(38) at $\sqrt{s} = 200$ GeV and $\sqrt{s} = 500$ GeV for the photon energy $E_\gamma > 1$ GeV and angular cuts of (39). Uncertainties of the last digits are given in parentheses.

Reaction	σ (200 GeV)	σ (500 GeV)
$e^+e^- \to e^+e^-\pi^+\pi^-$	100.6(3) fb	21.7(1) fb
$e^+e^- \to e^+e^-\pi^+\pi^-\gamma$	9.03(9) fb	2.33(4) fb
$e^+e^- \to e^+e^-\mu^+\mu^-\pi^+\pi^-$	27.1(4) ab	7.72(12) ab
$e^+e^- \to e^+e^-\mu^+\mu^-\pi^+\pi^-\gamma$	4.18(6) ab	1.47(3) ab
$e^+e^- \to be^+\nu_e\bar{b}e^-\bar{\nu}_e$	25.1(2) ab	6.734(8) fb
$e^+e^- \to be^+\nu_e\bar{b}e^-\bar{\nu}_e\gamma$	1.96(2) ab	1.559(4) fb
$e^+e^- \to e^+e^-\mu^+\mu^-\tau^+\tau^-\pi^+\pi^-$	0.0078(1) ab	0.0034(1) ab
$e^+e^- \to e^+e^-\mu^+\mu^-\tau^+\tau^-\pi^+\pi^-\gamma$	0.00168(5) ab	0.00085(4) ab

$$e^+e^- \to be^+\nu_e\bar{b}e^-\bar{\nu}_e\gamma, \tag{36}$$

$$e^+e^- \to e^+e^-\mu^+\mu^-\tau^+\tau^-\pi^+\pi^-, \tag{37}$$

$$e^+e^- \to e^+e^-\mu^+\mu^-\tau^+\tau^-\pi^+\pi^-\gamma \tag{38}$$

at $\sqrt{s} = 200$ GeV and $\sqrt{s} = 500$ GeV for $E_\gamma > 1$ GeV and with the following angular cuts on the photon–beam $\theta(\gamma, \text{beam})$, lepton–beam $\theta(l, \text{beam})$, pion–beam $\theta(\pi, \text{beam})$, photon–lepton $\theta(\gamma, l)$, photon–pion $\theta(\gamma, \pi)$, lepton–pion $\theta(l, \pi)$ and lepton–lepton' $\theta(l, l')$, $l \neq l'$, angles:

$$5^\circ < \theta(\gamma, \text{beam}),\ \theta(l, \text{beam}),\ \theta(\pi, \text{beam}) < 175^\circ, \qquad \theta(\gamma, l),\ \theta(\gamma, \pi),\ \theta(l, \pi),\ \theta(l, l') > 5^\circ, \tag{39}$$

are shown in Table 4, Predictions for reactions with the $\pi^+\pi^-$-pair in the final state, which are probably much more interesting at low energy e^+e^- colliders, have been derived here within a simple scalar QED model. Reactions (35) and (36) are interesting for investigating the top-quark pair production and decay in the e^+e^- collider. In the LO of SM in the unitary gauge and with the neglect of e^+e^-–Higgs boson coupling, they receive contributions from 1 306 and 11 124 Feynman diagrams, respectively. Note that reaction (36) at $\sqrt{s} = 500$ GeV receives contributions from peaks due to t- and $\bar{t}$-quark, W^+ and W^- bosons exchanged in the s-channel, the t-channel peaks due to presence of e^+e^--pair in the final state and the energy and collinear peaks due to the photon radiation. The small MC error of the corresponding cross section shows that the current version of `carlomat` is capable to handle all those peaks simultaneously. However, thorough tests of the results presented in Table 4 against programs by other authors [5–10] would require some dedicated effort and are beyond the scope of the present work. Some cross sections listed in Table 4 are so small that they are much below feasibility of any future collider project. They have been presented just to demonstrate the potential of `carlomat` in finding predictions for reactions with rather huge numbers of the Feynman diagrams, as e.g. reaction (38) which receives contributions from 262 920 Feynman diagrams in the LO. It should be noted that the cross sections of radiative reactions presented in Table 4, as well as those of Table 2, depend strongly on the photon energy cut. To cancel the dependence one should combine them with the $O(\alpha)$ virtual corrections to corresponding nonradiative reactions, which is beyond the scope of `carlomat`.

4. Summary

Announced already some time ago [25], a new version of the general purpose MC program `carlomat` that substantially improves efficiency of the phase space integration by automatic inclusion of parameterizations which map away the t-channel poles and peaks due to soft and collinear photon or gluon emission, has been presented. It also includes the QP versions of the routines for computation of the helicity amplitudes and phase-space parameterizations the calls to which have been implemented in the code generation part of the program. The QP arithmetics allows to control better numerical stability of computations performed with `carlomat`. Moreover, a new option of generating the s-channel kinematics, whose compilation and execution in the former versions of the program might be quite time consuming, has been added. The new s-channel kinematics is much shorter and hence speeds up both the compilation and execution time of the MC programs. The main routine of the MC computation part of the program has been supplemented with the MPI in order to allow for a parallel run on several processor cores.

As all former versions `carlomat_4.0` is distributed as a single `tar.gz` archive `carlomat_4.0.tgz` which can be downloaded from the CPC Program Library or from http://kk.us.edu.pl/carlomat.html. All the necessary instructions for preparation and running of the program can be found in file `instructions.pdf` included in the distribution. We only note here that the MPI version of the MC program can be run with the command

```
make -f mpi mc,
```

where `mpi` is the corresponding makefile. The latter should be priorly edited and the variables at the top of it, which specify the number of processor cores, name of the Fortran compiler and compilation options, set to appropriate values, e.g.

```
n_cores:=2
FF=mpif90
FFLAGS=-O.
```

Declaration of competing interest

I declare that I have no known competing financial interests or personal relationships that could have appeared to influence the work reported in this paper.

Appendix A. Supplementary material

Supplementary material related to this article can be found online at https://doi.org/10.1016/j.cpc.2022.108330.

References

[1] FCC Collaboration, A. Abada, et al., Eur. Phys. J. C 79 (2019) 474;
FCC Collaboration, A. Abada, et al., Eur. Phys. J. Spec. Top. 228 (2019) 261;
FCC Collaboration, A. Abada, et al., Eur. Phys. J. Spec. Top. 228 (2019) 755.

[2] M. Aicheler, et al. (Eds.), A Multi-TeV Linear Collider Based on CLIC Technology: CLIC Conceptual Design Report, CERN, 2012;
CLIC CLICdp Collaborations, P. Roloff, et al., The compact linear e^+e^- collider (CLIC): physics potential, arXiv:1812.07986 [hep-ex];
CLICdp CLIC Collaborations, P.N. Burrows, et al., The Compact Linear Collider (CLIC) – 2018 Summary Report, CERN Yellow Rep. Monogr., vol. 1802, 2018, pp. 1–98, arXiv:1812.06018 [physics.acc-ph], CERN-2018-005-M;
L. Linssen, et al., Physics and detectors at CLIC: CLIC conceptual design report, https://doi.org/10.5170/CERN-2012-003, arXiv:1202.5940 [physics.ins-det], 2012;
T.K. Charles, et al., CLICdp, CLIC, The compact linear collider (CLIC) - 2018 summary report, in: P.N. Burrows, et al. (Eds.), CERN Yellow Rep. Monogr., vol. 1802, 2018, arXiv:1812.06018 [physics.acc-ph];
P. Roloff, et al., CLIC, CLICdp, The compact linear e^+e^- collider (CLIC): physics potential, arXiv:1812.07986 [hep-ex], 2018.

[3] T. Behnke, J.E. Brau, B. Foster, J. Fuster, M. Harrison, et al., The international linear collider technical design report - volume 1: executive summary, arXiv:1306.6327;
H. Baer, T. Barklow, K. Fujii, Y. Gao, A. Hoang, et al., The international linear collider technical design report - volume 2: physics, arXiv:1306.6352.

[4] CEPC Study Group, CEPC conceptual design report: volume 1 – accelerator, arXiv:1809.00285 [physics.acc-ph];
CEPC Study Group, CEPC conceptual design report: volume 2 — physics & detector, arXiv:1811.10545 [physics.acc-ph].

[5] T. Stelzer, W.F. Long, Comput. Phys. Commun. 81 (1994) 357;
F. Maltoni, T. Stelzer, J. High Energy Phys. 02 (2003) 027;
J. Alwall, M. Herquet, F. Maltoni, O. Mattelaer, T. Stelzer, J. High Energy Phys. 06 (2011) 128;
H. Murayama, I. Watanabe, K. Hagiwara, KEK-91-11.

[6] A. Pukhov, et al., arXiv:hep-ph/9908288;
E. Boos, et al., Nucl. Instrum. Methods A 534 (2004) 250;
A. Belyaev, N.D. Christensen, A. Pukhov, Comput. Phys. Commun. 184 (2013) 1729.

[7] M.L. Mangano, M. Moretti, F. Piccinini, R. Pittau, A. Polosa, J. High Energy Phys. 0307 (2003) 001.

[8] A. Kanaki, C.G. Papadopoulos, Comput. Phys. Commun. 132 (2000) 306;
C.G. Papadopoulos, Comput. Phys. Commun. 137 (2001) 247;
A. Cafarella, C.G. Papadopoulos, M. Worek, Comput. Phys. Commun. 180 (2009) 1941.

[9] T. Gleisberg, et al., J. High Energy Phys. 0402 (2004) 056;
T. Gleisberg, et al., J. High Energy Phys. 0902 (2009) 007;
T. Gleisberg, S. Höche, J. High Energy Phys. 0812 (2008) 039.

[10] M. Moretti, T. Ohl, J. Reuter, arXiv:hep-ph/0102195;
W. Kilian, T. Ohl, J. Reuter, Eur. Phys. J. C 71 (2011) 1742.

[11] K. Kołodziej, Comput. Phys. Commun. 180 (2009) 1671.

[12] K. Kołodziej, Comput. Phys. Commun. 185 (2014) 323.

[13] K. Kołodziej, Comput. Phys. Commun. 196 (2015) 563;
K. Kołodziej, `carlomat_3.1`, http://kk.us.edu.pl/carlomat.html.

[14] J. Küblbeck, M. Böhm, A. Denner, Comput. Phys. Commun. 60 (1990) 165;
T. Hahn, Nucl. Phys. Proc. Suppl. 89 (2000) 231;
T. Hahn, Comput. Phys. Commun. 140 (2001) 418.

[15] H. Tanaka, T. Kaneko, Y. Shimizu, Comput. Phys. Commun. 64 (1991) 149;
F. Yuasa, et al., Prog. Theor. Phys. Suppl. 138 (2000) 18;
G. Belanger, et al., Phys. Rep. 430 (2006) 117.

[16] J. Alwall, et al., J. High Energy Phys. 07 (2014) 079, arXiv:1405.0301 [hep-ph].

[17] E. Bothmann, et al., SciPost Phys. 7 (2019) 034, arXiv:1905.09127 [hep-ph].

[18] G. Bevilacqua, et al., Comput. Phys. Commun. 184 (2013) 986.

[19] K. Kołodziej, M. Zrałek, Phys. Rev. D 43 (1991) 3619.

[20] F.A. Berends, C.G. Papadopoulos, R. Pittau, Comput. Phys. Commun. 136 (2001) 148.

[21] K. Kołodziej, F. Jegerlehner, Comput. Phys. Commun. 159 (2004) 106.

[22] M. Luscher, Comput. Phys. Commun. 79 (1994) 100;
F. James, Comput. Phys. Commun. 79 (1994) 111.

[23] F.A. Berends, R. Pittau, R. Kleiss, Comput. Phys. Commun. 85 (1995) 437, arXiv:hep-ph/9409326.

[24] A. Denner, S. Dittmaier, M. Roth, D. Wackeroth, Nucl. Phys. B 560 (1999) 33, arXiv:hep-ph/9904472.

[25] K. Kołodziej, Acta Phys. Pol. B 50 (2019) 1971.